THE GAS PHASE OXIDATION OF ACETALDEHYDE REACTION MECHANISM AND KINETICS

D. L. Trimm and K. Hessam

School of Chemical Engineering and Industrial Chemistry, University of New South Wales Kensington NSW 2033, Australia; and Department of Chemical Engineering and Chemical Technology, Imperial College of Science and Technology, The University of London, England

Abstract The mechanism of the low temperature oxidation of gaseous acetaldehyde was investigated in the temperature range of 150-400°C. The minor, intermediate and major products were identified and measured quantitatively by sampling directly into the ionization chamber of an MS10-C2 mass spectrometer from the reactor. The formation of H_2O, CO, CO_2, HCOOH, H_2, HCHO, CH_3COOH and CH_3OH as the major products, the presence of H_2O_2, $(CH_3)_2CO$, $(CH_3CO)_2O_2$, $(CH_3CO)_2$ and CH_4 as the minor products, the production of the unstable product CH_3OOH and the existence of peracetic acid as a degenerate branching intermediate were confirmed. The exprimental results led to a proposed degenrate branched chain mechanism for the gas-phase oxidation of acetaldehyde. This paper attempts to explain the kinetics in the region of lower slow combustion (at 150°C), cool flames, and upper slow combustion (at 400°C) with an initial total pressure between 4 to 12 cm. Hg. The major products detected were (in order of concentrations): $H_2O > CO > CO_2 > H_2 > CH_3COOH > HCHO > HCOOH$ The reaction orders obtained were 0.38 with respect to oxygen pressure and 1.85 with respect to acetadehyde pressure for maximum rate. The reaction rate was found to be independent of the total pressure. In temperature range of 150-250°C, the reaction was accompanied by a pressure decrease, while in 275-400°C, a pressure increase was observed. The low activation energies of 53.50 KJ $mole^{-1}$ (in 150-250°C region) and 57 KJ $mole^{-1}$. (in 275-400°C region) indicate that the reaction is a degenerate branching chain type for which the net-branching factor is correlated with the acetaldehyde pressure and the activation energy as $\phi = K\,[P_{CH_3CHO}]^{0.8}\exp[-E/RT]$. The kinetics data obtained by the mass spectrometer were analyzed by computer programing and the results were presented by the appropriate kinetics plots.

Key Words Combustion, Thermal Oxidation, Degenerate Branching, Organic Fuels, Induction Period

چکیده واکنش اکسیداسیون استالدئید گازی در دماهای ۱۵۰-۴۰۰ درجه سانتیگراد در یک سیستم ثابت بوسیله تجزیه با دستگاه اسپکترومتر جرم، بررسی شده است. مطالعات این واکنش جهت مکانیزم و سینیتیک در ناحیه اکسیداسیون آهسته (۱۵۰ °C) و شعله سرد و ناحیه دمای بالا (۴۰۰ °C) بوده است. فرآورده های فرعی واسطه ای و همچنین فرآورده های نهائی از نظر کیفی و کمی بوسیله تجزیه مخلوط راکتور شناخته و اندازه گیری شده است. تشکیل H_2O ، CO ، CO_2 ، H_2 ، HCOOH ، HCHO ، CH_3COOH و CH_3OH بعنوان فرآورده های اصلی و H_2O_2 ، $(CH_3)_2CO$ ، $(CH_3CO)_2O_2$ ، $(CH_3CO)_2$ و CH_4 بعنوان فرآورده های فرعی و تشکیل و مصرف پراستیک اسید بعنوان ترکیب واسطه ای تخریبی برای تولید انشعابهای زنجیری، مطالعه گردیده است. درجه واکنش برای سرعت ماکزیمم نسبت به اکسیژن ۰/۳۸ و نسبت به استالدئید ۱/۸۵ می‌باشد ودر فاصله دمائی ۱۵۰-۲۵۰°C واکنش با کاهش فشار و در فاصله دمائی ۲۷۵-۴۰۰°C واکنش با افزایش فشار همراه بوده است. انرژیهای فعالیت پایین برای این واکنش (KJ/mole ۵۳/۵۰ در °C ۲۵۰-۱۵۰) و (KJ/mole ۵۷/۲۷ در °C ۴۰۰-۲۷۵) نشان می دهد که واکنش مزبور در شرایط بالا از نوع زنجیری انشعابی تخریبی با ضریب انشعابی ϕ بوده بطوریکه ثابت سرعت و فشار گاز استالدئید و دما، انرژی فعالیت در رابطه زیر هم بستگی دارد: $\phi = K\,[P_{CH_3CHO}]^{0.8}\exp(-E/RT)$ مقادیر سینیتیکی بدست آمده بوسیله مطالعه اسپکترومتری جرم برای محاسبات کامپیوتری، برنامه نویسی شده و نتایج عددی مربوطه بصورت دیاگرام، رسم گردیده است.

INTRODUCTION

The combustion process involves a number of chemical reactions which depends on the nature of the fuel used, the conditions of the system and several variable factors affecting the process by which one or more reaction steps may be controlled.

In chemistry combustion commences with the occurance of self-supporting exothermic reactions. Combustion leads to several outcomes. One such effect is detonation wave which is produced from the chemical energy with a rate dependent on the temperature and pressure. The light emission is another chemical effect dependent on specific chemical processes. The physical processes involved in combustion are those related to mass and energy transfer.

In a static system of combustion, two regions with different reaction behaviors, which depend primarily on the temperature and pressure and are separated by a boundary may be distinguished. On one side of the boundary the reaction is slow, while on the other side explosion occurs. For hydrocarbon fuels, the situation is more complex. There is a sharp boundary at which true ignition occurs with a yellow flame and several individual phenomena. Although the combustion phenomena are characterized by various mechanistic reactions, the process under less extreme conditions is known as slow combustion, where the pressure in the system pulses at a certain time but does not lead to a true ignition.

The practical application of the combustion of organic fuels in particular hydrocarbons is the production of either energy or chemicals.

As the experimental observations indicate, during the early stages of the slow combustion of hydrocarbons, the chain branching is developed via the production of the reaction intermediates such as aldehydes and peroxides, where these compounds undergo individual specific reactions (i.e. homogenous dissociation, isomerization and eventually branching) to propagate the chain. Thus, the improtance of the role of aldehydes particularly acetaldehyde in the hydrocarbon/oxygen systems would be obvious.

Gaseous acetaldehyde is relatively stable at moderate temperatures but a trace of oxygen accelerates its decomposition [1]. The intermediate oxidation products in the lower slow combustion zone are mainly peroxides which decompose to produce more reactive free radicals . At the cool-flame boundary (240-335°C) the pressure decrease in the system is gradually changed to an-increase due to the instability of peroxides (e.g. peracid). In the upper slow combustion region, the reaction starts with a rapid pressure increase due to rapid branching via decomposition of peroxy intermediates. The oxidation products obtained were analyzed by the study of the mass peaks in the range of 1-200.

The kinetics study of gas phase oxidation of acetaldehyde in three combustion zones, namely the lower slow combustion region, the cool flame region and the upper slow combustion region has been carried out in the temperature range of 150-400°C and at varying initial reactant pressures.

The disappearance of reactants and formation of the intermediates with their decomposition and also the production of the final major and minor products were monitored continuously by using individual pure compounds.

EXPERIMENT

Pure gaseous acetaldehyde was prepared by vacuum distillation of a 99% pure liquid acetaldehyde (B. D. H.). The acetaldehyde was first carefully degassed, and then condensed into the storage trap. To introduce a sample into the clean pyrex glass reactor, the storage trap was first warmed to room temperature and the first few portions of gas were rejected, then a

portion of gas was admitted through a spiral pressure gauge into the reaction vessel. The connecting glass tubes, taps and spiral gauge were electrically heated to a temperature of 120°C to avoid any gas condensation, and the whole apparatus was evacuated to (2-4)10^{-4} mm. Hg to prevent any oxygen absorption by acetaldehyde.

The gaseous mixture of unused reactants and products was admitted directly into the ionization chamber of the mass spectrometer through a small hole at the reactor exit. The instrument was first calibrated by using pure compounds as follows:

Acetaldehyde (analar grade) was prepared from Hopkin and Williams company. Pure oxygen (nitrogen free O_2) was prepared from the British Oxygen Company in the cylinders. The purity of this gas was being monitored at intervals by the qualitative mass spectrometric analysis.

Liquid hydrogen peroxide (Laporte Ind.), peracetic acid (by vaporization of a 72% pure liquid), formic acid, acetic acid. Water and methanol (by vacuum distillation of liquid), hydrogen gas (from cylinders) and formaldehyde (by vaccum distillation of paraformaldehyde) and methane prepared, measured by the sensitive pressure gauge and then injected into the instrument to obtain the relevant mass peaks.

The reaction vessel (capacity = 171cm^3) was made of pyrex glass in the form of an open hook shape and sealed off at the bent end. The open end was connected to the sampling glass tube, and a probe with a hole was joined to the hook and passed through the furnace wall to a glassmetal sealed leak point into the ion source of the mass spectrometer (Figure 1).

The reactor pressure varied from 10 to 200 mm Hg, while the ion source could only be operated at pressures below 10^{-4} mm Hg. To obtain a linear relation between the gas pressure in the reactor and the peak height in its cracking pattern, it was necessary to maintain the concentration of the gas in the reactor at a constant fraction of its concentration in the

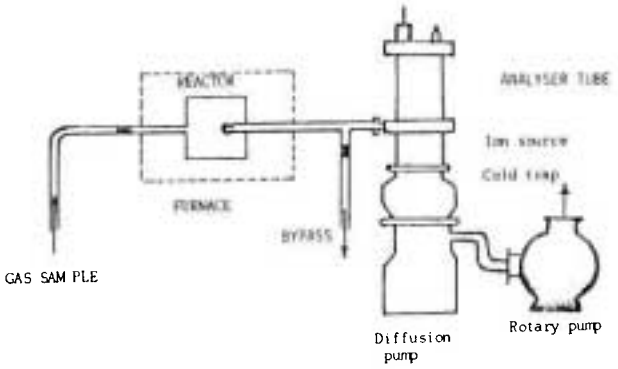

Figure 1. A schematic diagram of mass spectrometer system.

ionization chamber [2, 3]. In this manner, the mass spectra obtained were satisfactory for quantitative measurements.

The reactor was suspended in an air oven heated electrically and insulated at the walls against heat loss. The temperature was controlled by a temperature indicating controller governed by a chromel-alumel thermocouple to within ± 2°C. The reaction mixture was continuously sampled through the hole into the instrument and it was possible to elucidate the reaction mixture composition at a given time.

RESULTS AND DISCUSSION

A set of peak time curves for a typical oxidation of gaseous acetaldehyde is shown in Figures 2 and 3. The contributing compounds found in the reaction mixture are presented in Table 1. In the slow combustion region, under the experimental conditions, the major products were indentified as H_2O, CO, CO_2, H_2, CH_3CO_2H, CH_2O and HCO_2H; the minor products were H_2O_2, CH_3OH, CH_4, $(CH_3)_2CO$, $(CH_3CO)_2$ and $(CH_3CO)_2O_2$ and the intermediate products were found to be CH_3CO_3H and CH_3O_2H. The decreasing mass peaks 29 and 43 indicate the acetaldehyde consumption and that at 32 shows the decrease in oxygen. The increasing mass peaks 2, 18, 28, 30, 44, 46 and 60 indicate the formation of hydrogen, water, carbon monoxide, formaldehyde,

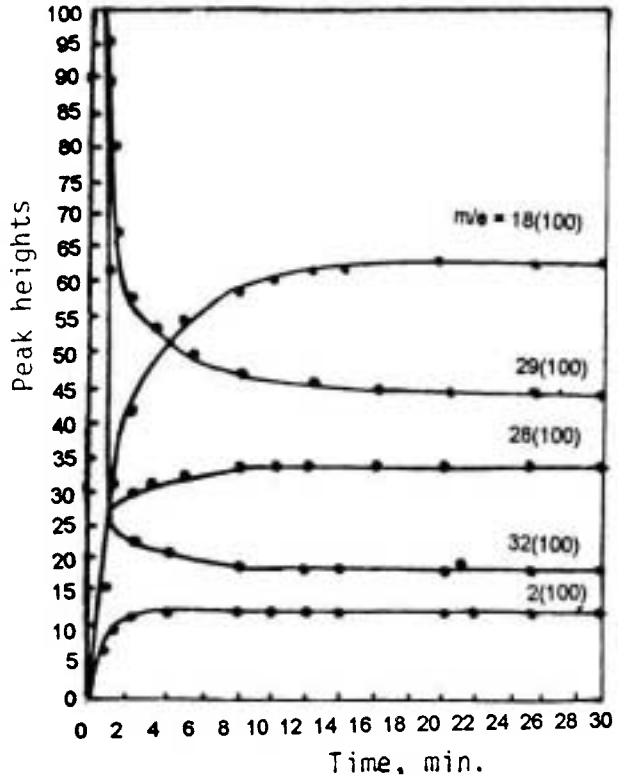

Figure 2. Mass peak height-time curves in the acetaldehyde-oxygen system. Initial CH_3CHO=40; O_2=45 mm.Hg. T= 300°C.

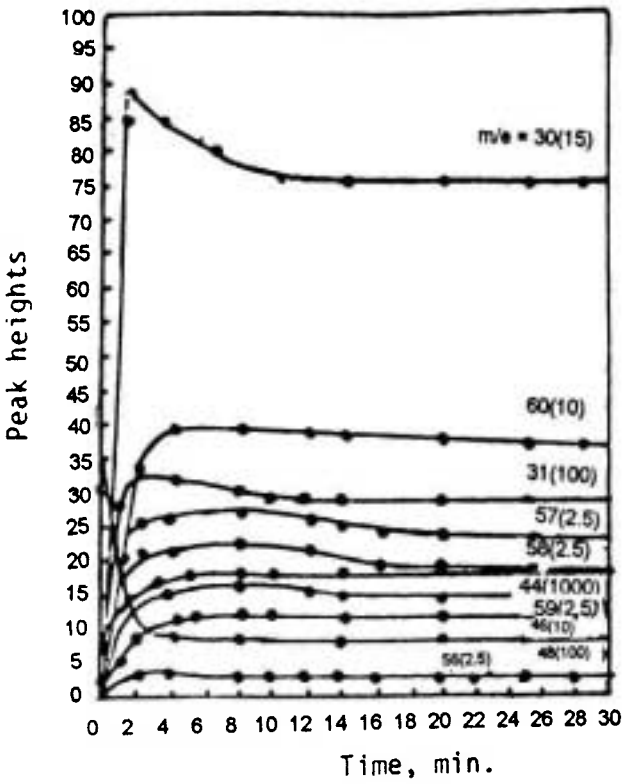

Figure 3. Mass peak height-time curves in the acetaldehyde-oxygen system. Initial CH_3CHO=40 mm.Hg. O_2=45 mm.Hg.

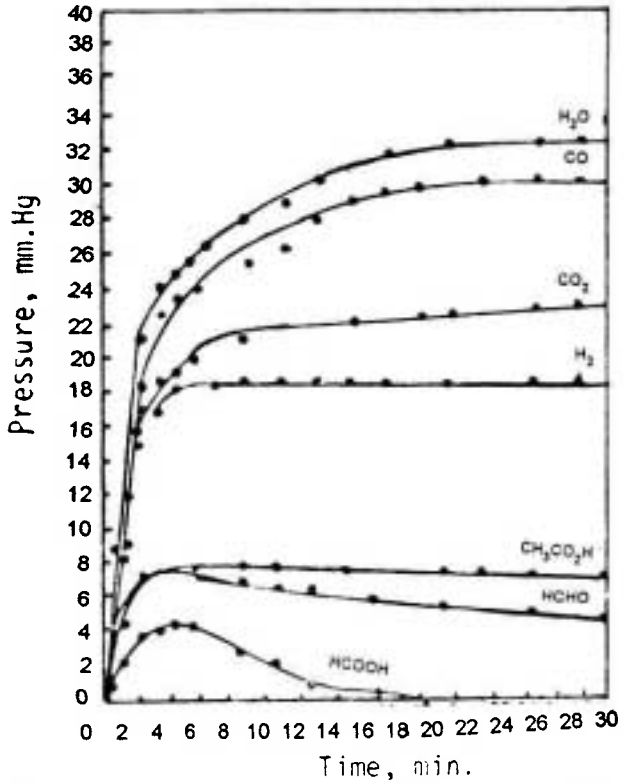

Figure 4. The pressure-time curves of the products in the gas-phase oxidation of acetaldehyde at 300°C. Initial O_2 = 45; CH_3CHO = 40 mm.Hg.

carbon dioxide, formic acid and acetic acid respectively as the major products, where the increasing mass peaks 16, 31, 58 and 86 show the formation of methane, methanol, acetone and biacetyl as minor products. The pressure-time curves for the products formed are shown in Figure 4.

The formation and decomposition of peroxides are indicated by mass peak-time curves (Figure 5). For hydrogen peroxide m/e = 34, methyl hydroperoxide m/e = 47 and 48, paracetic acid m/e = 74, 75, 76 and 77, and diacetyl peroxide m/e = 118. These figures were obtained after subtracting the background peaks of the instrument and the contributions of oxygen and other compounds. The concentration of peroxides formed during the reaction course are indicated in Figure 6.

To investigate the behavior of all peroxides in the ion source of the mass spectrometer and to obtain the cracking patterns of these compounds, a number of

TABLE 1. Superimposed Mass Spectrum Contributions of Acetaldehyde Oxidation

(m/e) Mass Number	Formula	Contributing components
2	H^+_2	Hydrogen
16	O^+	Oxygen, carbon dioxide, methane
17	OH^+	Hydroxyl radical, formic acid, steam
18	H_2O^+	Steam, methanol, acetaldehyde
27		Acetaldehyde
28	CO^+	Carbon monoxide, carbon dioxide, acetaldehyde, acetic acid, formic acid, methanol formaldehyde, oxygen
29	$\cdot HCO^+$	Fromyl radical, formaldehyde, acetaldehyde, acetic acid, formic acid, methanol, carbon monoxide, carbon dioxide
30	CH_2O^+	Formaldehyde, carbon monoxide, formic acid, carbon dioxide, acetaldehyde, methanol
31	CH_3O^+	Methanol, acetic acid, formic acid
32	O^+_2,CH_4O^+	Oxygen, formic acid, methanol
33	HO2+	Hydroperxyl radical, hydrogen peroxide, methanol, oxygen
34	$H_2O_2^+$	Hydrogen peroxide, oxygen
42	$C_2H_2O^+$	Acetaldehyde, acetic acid
43	$C_2H_3O^+$	Acetyl radical, acetaldehyde, acetic acid
44	CO_2^+,$C_2H_4O^+$	Carbon dioxide, acetaldehyde, acetic acid, formic acid, oxgyen
45	$C_2H_5O^+$,CO_2H^+	Acetaldehyde, carbon dioxide, formic acid, acetic acid
46	$CH_2O_2^+$,$C_2H_6O^+$	Formic acid, acetaldehyde
47	$CH_3O_2^+$	Methyl hydroperoxide
48	$CH_4O_2^+$	Methyl hydroperoxide
57		Acetone
58	$(CH_3)_2CO^+$	Acetone
59		Acetone
60	$C_2H_4O_2^+$	Acetic acid
75	$C_2H_3O_3^+$	Peracetyl radical, peracetic acid
76	$C_2H_3O_3^+$	Peracetic acid

peroxides were partially purified by vacuum fractionation and injected into the preheated (60-90°C) reactor. A mass balance was performed to examine the accuracy of the measurement of the major products and found satisfactory (Table 2). In all cases, the mass-peak scanning was carried out at

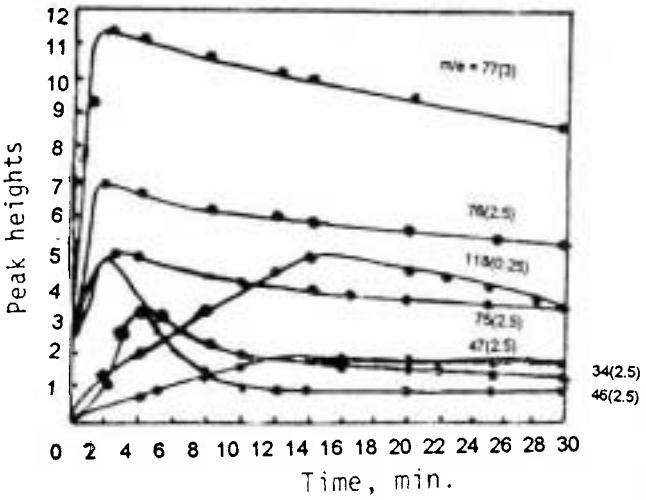

Figure 5. Mass peak height-time curves of peroxidic products in acetaldehyde-oxygen system at 300°C.

high sensitivities. To avoid any explosive decomposition of peroxides, the samples were not completely purified and suitable conditions were used in the reactor (low pressures and temperatures). Although the samples were not too pure, under the

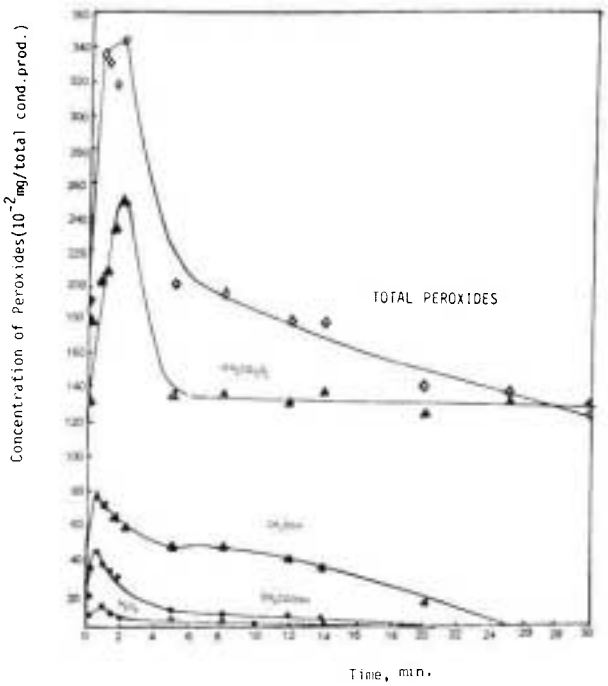

Figure 6. Concentration-time curves of peroxidic products in the oxidation of gaseous acetaldehyde at 300°C. Initial CH_3CHO = 40 ; O_2 = 45 mm.Hg. Reaction vessel: clean pyrex glass, dia. = 28.4 mm. volume = 171 ml.

TABLE 2. Mass Balance of the Reaction Mixture (Time of Analysis = 12 minutes)

Reactants	**C (mm.Hg.)**	**H (mm.Hg.)**	**0 (mm.Hg.)**
Acetaldehyde used	72.2	144.4	36.1
Oxygen used	-	-	89.5
Total Reactants	72.2	144.4	125.6
Products	**C (mm.Hg.)**	**H (mm.Hg.)**	**0 (mm.Hg.)**
HCOOH	1	2	2
HCHO	6.95	13.90	6.95
CH_3COOH	15.76	31.52	15.76
H_2	-	37.02	-
CO_2	21.90	-	43.80
H_2O	-	60.80	30.40
CO	28.14	-	28.14
Total	73.75	145.24	127.05
Difference	+1.55	+0.84	+1.45
Error%	+2.14	+0.51	+1.15

conditions selected, the relatively small parent peaks obtained in the mass spectrum were sufficient to study the characteristics of these compounds in the ionisation chamber. Di-t-butylperoxide was used as a stable reference since under the conditions applied the parent peak showed a relatively high values compared with those of other peroxides. Hydrogen peroxide, peracetic acid and biacetyl peroxide were used to obtain their cracking patterns as references.

The identification of peroxides [4], both the formation and role of the peroxides in the aldehyde/O_2 systems have been points of interest in combustion chemistry. The study of the reaction mechanism should elucidate the nature of the propagation stages through which the chain reaction proceeds. The formation of peroxidic compounds during the slow combustion of both hydrocarbons and aldehydes would necessitate the idenfitication of these products and the distinction between those formed by peroxidation process of hydrocarbons, and those produced from the aldehyde oxidiation reaction.

The idenfitication of peroxides either in the RH/O_2 or RCHO/O_2 systems has been confirmed by iodometric method as a rapid test for comparing the qualitative and quantitative results with those obtained by the mass spectral data. The concentration of peroxide was then calculated by considering the volume of sodium thiosulphate solution used to react with the liberated iodine from peroxide and potassium iodide solution under experimental conditions (temperature, solubility and time of contact). Figure 6 shows the accumulation and decomposition of peroxides. The hydrogen peroxide concentration increases to a small maximum value, after which it decreases slightly to a steady value. Peracetic acid and methyl hydroperoxide formation are rather faster. The maximum concentrations are attained within the first minute of reaction and then decrease sharply. Biacetyl peroxide accumulates up to the second minute of reaction, after which it decreases to a steady

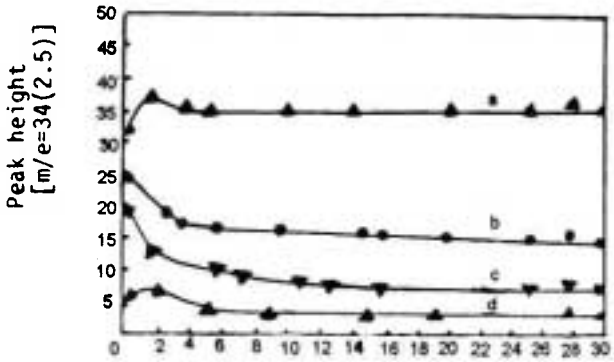

Curve	Initial CH_3CHO (mm.Hg)
a	10
b	20
c	30
d	50

Figure 7. Variation of mass peak m/e = 34 with time at 300°C. Initial O_2 = 45 mm.Hg.

concentration.

The peroxides produced in the reaction were H_2O_2, CH_3O_2H, CH_3CO_3H and $CH_3CO\text{-}OO\text{-}OCCH_3$. Hydrogen peroxide and biacetyl peroxide remained as final peroxidic products. The formation and decomposition of hydrogen peroxide in various acetaldehyde-oxygen mixtures is shown in Figure 7. It can be observed that the higher the aldehyde initial pressure, the lower the maximum rate of H_2O_2 production (peak height at m/e = 34), but the rate of H_2O_2 decomposition is almost the same for all aldehyde pressures, presumbaly because of the reaction $H_2O_2 \xrightarrow{wall} H_2O + \frac{1}{2}O_2$.

Plots of mass peak 47 against time for various acetaldehyde initial pressures are given in Figure 8. Curves a-d indicate a higher maximum accumulation and more rapid decomposition of methyl hydroperoxide for higher fuel pressure. The rate of methyl hydroperoxide decomposition is in the order a>b>c>d, which is identical to the initial aldehyde pressures. The variation of mass peak 48 against time has very similar characteristics, since both mass

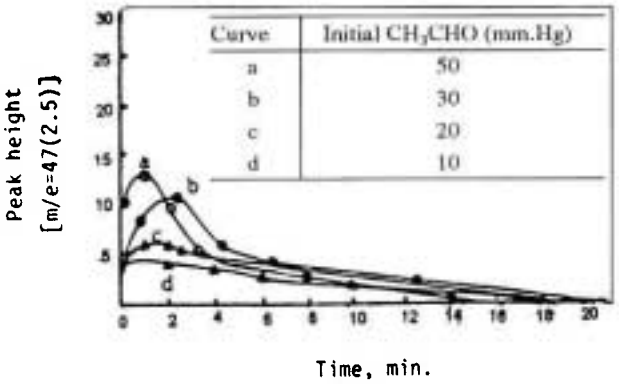

Figure 8. Variation of mass peak m/e = 47 with time at 300°C. Initial O_2 = 45 mm.Hg.

peaks 47 and 48 represent ion fragments of methyl hydroperoxide. The homogeneous decomposition of this intermediate product yields branching:

$$CH_3OOH \rightarrow CH_3\dot{O} + \dot{O}H$$

which is endothermic with an activation energy [5] of about 134 kJ mole^{-1}. Plots of mass peak 76 against time for varying fuel pressures (Figure 9) indicate a lower maximum accumulation and more rapid decomposition of peracetic acid for higher aldehyde initial pressure. Both mass peaks 75 and 76, together with a considerable contribution of mass peak 60, represent ion fragments of peracetic acid, which is the earliest oxidation product in CH_3CHO/O_2 system. The mass peak height-time curves of peroxides identified in the oxidation mixture (Figures 10 and

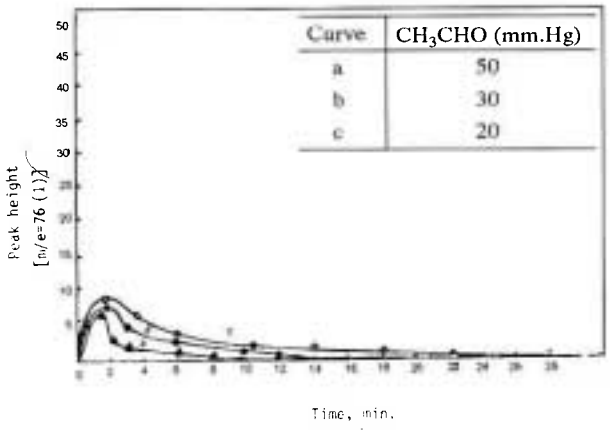

Figure 9. Variation of mass peak m/e = 76 with time at 300°C. Initial O_2 = 45 mm.Hg.

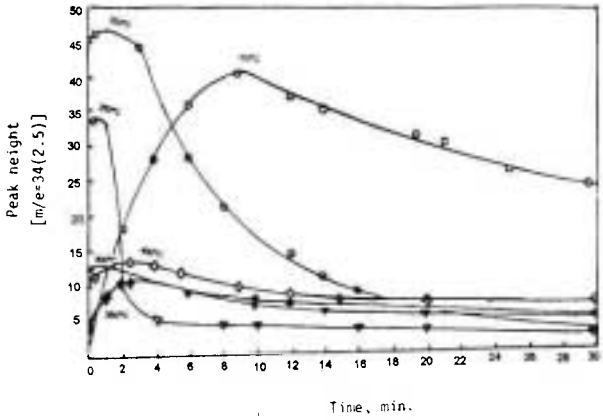

Figure 10. Variation of mass peak 34 with time at various temperatures. Initial CH_3CHO = 40 ; O_2 = 45 mm.Hg.

13) show that the retes of formation and decompositions of hydrogen peroxide and biacetyl peroxide increase with temperature, but their maximum concentrations show no regularity with temperature change. Such regularity has been observed, however, for methyl hydroperoxide and peracetic acid (Figures 11 and 12). The formation of CH_3OOH and CH_3COOOH will be faster at a higher temperature than at a lower temperature, but the maximum concentrations attained, decrease with a temperature rise, which means higher consumption of these peroxides.

Inspection of the decomposition rates of methyl hydroperoxide and peracetic acid (acetyl

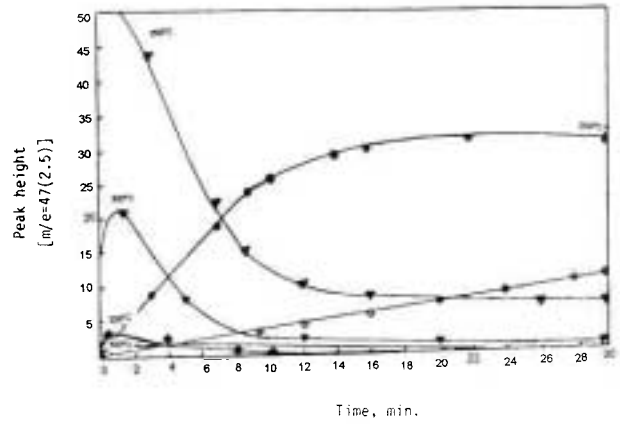

Figure 11. Variation of mass peak 47 with time at various temperatures. Initial CH_3CHO = 40 ; O_2 = 45 mm.Hg.

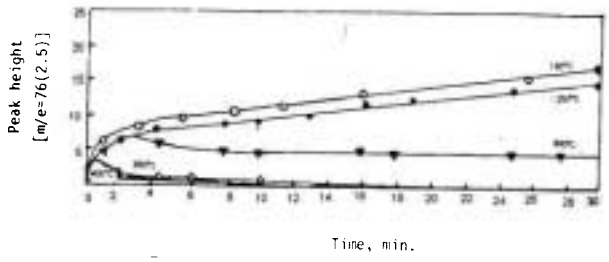

Figure 12. Variation of mass peak 76 with time at various temperatures. Initial $CH_3CHO = 40$; $O_2 = 45$ mm.Hg.

hydroperoxide), which are accelerated by an increase in initial fuel pressure, indicates the probable responsibility of these origanic peroxides for degenerate branching in the gas phase oxidation of acetaldehyde at low temperatues [6, 7, 8, 9]. The branching reaction of peracetic acid is thought to involve:

$$CH_3CO_3H \rightarrow CH_3CO_2H + \dot{O}$$
$$CH_3CO_3H \rightarrow CH_3\dot{C}O_2 + \dot{O}H$$

which is endothermic with on activation energy [1] of 63-92 kJ mole^{-1} followed by

$$CH_3\dot{C}O_2 \rightarrow \dot{C}H_3 + CO_2 \text{ (Exothermic) } E=32 \text{ kJ mole}^{-1}$$
$$CH_3\dot{C}O_2 \rightarrow CH_3\dot{O} + CO \text{ (Endothermic) } E=113 \text{ kJ mole}^{-1}$$

MECHANISTIC FEATURE

The intermediates and final products observed as

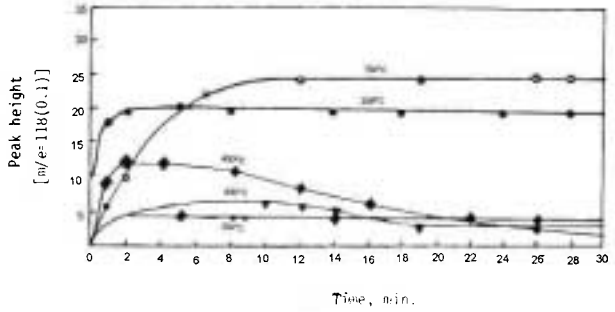

Figure 13. Variation if mass peak 118 with time at various temperatures. Initial $CH_3CHO = 40$; $O_2 = 45$ mm.Hg.

well as the kinetics measurement are examined in the light of reaction mechanism. The results indicate that the reaction almost certainly involves a degenerately branched chain process over the range 150-400°C in which a peracid and an alkyl hydroperoxide are the chain branching intermediates. The reaction can, perhaps, be best discussed in the light of a proposed mechanism.

The initiation step for all aliphatic aldehydes, probably involves a reaction such as

$$CH_3CHO + O_2 \rightarrow CH_3\dot{C}O + H\dot{O}_2 \qquad (i)$$

which has an endothermicity of about 170 kJ mole^{-1}. The produced acyl radicals undergo reaction with molecular oxygen to produce peracyl and alkyl proxy radicals:

$$CH_3\dot{C}O + O_2 \rightarrow CH_3C\dot{O}_3 \qquad (1)$$

$$CH_3\dot{C}O + O_2 \rightarrow CH_3\dot{O}_2 + CO \qquad (4)$$

Both reactions (i) and (1) are very rapid [10]. Peracyl radicals, $CH_3C\dot{O}_3$ may either abstract a hydrogen atom from the molecule to give the corresponding peracid, and/or decompose to form other radicals:

$$CH_3C\dot{O}_3 + CH_3CHO \rightarrow CH_3CO_3H + CH_3\dot{C}O$$

$$CH_3C\dot{O}_3 \rightarrow CH_2O + H\dot{C}O_2 \qquad (1a) \qquad (2)$$
$$CH_3C\dot{O}_3 \rightarrow CH_3\dot{O} + CO_2 \qquad (1a)$$

The produced radicals $H\dot{C}O_2$, $CH_3\dot{O}$ and $CH_3\dot{O}_2$ can abstract hydrogen atoms from acetaldehyde to give HCOOH, CH_3OH and CH_3OOH respectively, although methyl hydroperoxide could be formed by the following reactions:

$$CH_3\dot{C}O \rightarrow \dot{C}H_3 + CO \qquad (4a)$$

$$\dot{C}H_3 + O_2 \xrightarrow{RH} CH_3OOH \qquad (4b)$$

The experimental pressure-time curves of peroxides in the reaction mixture (Figures 5 and 6) show that the

decomposition of one or both of the intermediates, peracetic acid and methyl hydroperoxide, are probably responsible for branching:

$$CH_3CO_3H \rightarrow CH_3\dot{C}O_2 + \dot{O}H \quad (3)$$
$$CH_3CO_3H \rightarrow CH_3CO_2H + \dot{O}$$

$$CH_3OOH \rightarrow CH_3\dot{O} + \dot{O}H \quad (4c)$$

The activation energies for 3 and 4c have been reported to be 63-92 [1], and 134 [5] kJ mole^{-1} respectively. These values, together with the endothermicity of the reactions show that all three will probably occur although Reaction 3 will be preferred. Figures 8 and 9 give the rates of decompoisition of methyl hydroperoxide and peracetic acid for various initial pressures. The results show that

$$\frac{-d[CH_3CO_3H]}{dt} = K[CH_3CHO]^{2.2}$$

and $$\frac{-d[CH_3OOH]}{dt} = K[CH_3CHO]^{1.5}$$

The apparent rates of decomposition of peracetic acid and methyl hydroperoxide are about 0.228 mg/min and 0.143 mg/min respectively. This indicates that under the same conditions, peracids are more reactive than alkyl hydroperoxides in degenerate branching.

Interaction between acetaldehyde, and peracetic acid may also occur, possibly by two modes [10]:

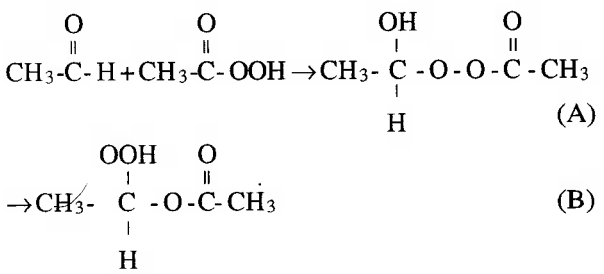

(A)

(B)

since compound (A) has a lower 0-0 dissociation energy than that of the parent peracid, the aldehyde-peroxide (A) is more likely [10]. The peroxide with structure (B) seems to have a bond dissociation energy about that of normal hydroperoxides.

Propagation of the chain probably involves the reactions:

$$CH_3\dot{C}O_2 + CH_3CHO \rightarrow CH_3COOH + CH_3\dot{C}O \quad (4d)$$

$$\dot{O}H + CH_3CHO \rightarrow H_2O + CH_3\dot{C}O \quad (5)$$

$$H\dot{O}_2 + CH_3CHO \rightarrow \dot{O}H + \text{products } (CO_2 + CH_4), (CO + CH_3OH) \text{ or } (CH_3CO_2H) \quad (6)$$

$$H\dot{O}_2 + CH_3CHO \rightarrow H_2O_2 + CH_3\dot{C}O \quad (7)$$

and termination steps may occur by one or more of the following reactions:

$$2CH_3\dot{C}O \rightarrow (CH_3CO)_2 \quad (8)$$

$$2CH_3\dot{C}O_3 \rightarrow (CH_3CO)_2O_2 + O_2 \quad (9)$$

$$CH_3\dot{C}O + CH_3\dot{C}O_3 \rightarrow (CH_3CO)_2O_2 \quad (10)$$

Biacetyl peroxide has been observed experimentally (Figures 5 and 6).

The proposed mechanism may be tested by kinetic analysis at the point of maximum rate, where the concentration of branching intermediate is maximal. Summarising the mechanism:

$$CH_3CHO + O_2 \rightarrow CH_3\dot{C}O + H\dot{O}_2 \quad (i)$$

$$CH_3\dot{C}O + O_2 \rightarrow CH_3C\dot{O}_3 \quad (1)$$

$$CH_3C\dot{O}_3 + CH_3CHO \rightarrow CH_3CO_3H + CH_3\dot{C}O \quad (2)$$

$$CH_3CO_3H \rightarrow \dot{O}H + CH_3C\dot{O}_2 (\dot{C}H_3 + CO_2) \text{ or } (CH_3\dot{O} + CO) \quad (3)$$

$$CH_3CO_3H + CH_3CHO \rightarrow \text{complex} \rightarrow \text{radicals} \quad (3a)$$

$$CH_3\dot{C}O + O_2 \rightarrow CH_3\dot{O}_2 + CO \quad (4)$$

$$CH_3\dot{C}O \rightarrow \dot{C}H_3 + CO \quad (4a)$$

$$\dot{O}H + CH_3CHO \rightarrow H_2O + CH_3\dot{C}O \quad (5)$$

$$H\dot{O}_2 + CH_3CHO \rightarrow \dot{O}H + \text{products } (CO_2 + CH_4), (CO + CH_3OH) \text{ or } (CH_3CO_2H) \quad (6)$$

$$H\dot{O}_2 + CH_3CHO \rightarrow H_2O_2 + CH_3\dot{C}O \quad (7)$$

$$2CH_3\dot{C}O \rightarrow \text{termination} \quad (8)$$

$$2CH_3C\dot{O}_3 \rightarrow \text{termination} \quad (9)$$

$$CH_3\dot{C}O + CH_3C\dot{O}_3 \rightarrow \text{termination} \quad (10)$$

Assuming that the branching and termination processes are to be by 3a and 9 respectively, the rates of production of different species may be found as follows:

$$x = (CH_3\dot{C}O) = \frac{-K_2^2 K_4 (CH_3CHO)^2}{K_9 (K_1 + K_4)(O_2)} = 0$$

$$y = (CH_3C\dot{O}_3) = \frac{-K_2 K_4 (CH_3CHO)}{K_9 (K_1 + K_4)}$$

$$z = (CH_3CO_3H) = \frac{-K_2^2 K_4 (CH_3CHO)}{K_{3a} K_9 (K_1 + K_4)}$$

$$\gamma = (\dot{O}H) = \frac{-K_i K_6 (O_2)}{K_5 (K_6 + K_7)}$$

$$u = (H\dot{O}_2) = \frac{K_i (O_2)}{(K_6 + K_7)}$$

The overall reaction rate can then be computed from the equation

$$W = \frac{-d(CH_3CHO)}{dt} = K_2(CH_3C\dot{O}_3)(CH_3CHO) + K_5(\dot{O}H) + K_5(\dot{O}H)(CH_3CHO) + (K_6 + K_7)(H\dot{O}_2)(CH_3CHO) + K_{3a}(CH_3CHO)(CH_3CO_3H)$$

Substituting the concentrations of the species as above and assuming $K_6 \cong K_7$,

$$W = \frac{-2K_2^2 K_4 (CH_3CHO)^2}{K_9 (K_1 + K_4)} + \frac{3}{2} K_i (CH_3CHO)(O_2)$$

since K_i is very small compared with K_2^2, the last term of this equation can be omitted to give

$$W = \frac{-2K_2^2 K_4 (CH_3CHO)^2}{K_9 (K_1 + K_4)}$$

with $K_1 << K_4$ the rate becomes

$$W = \frac{-2K_2^2}{K_9 K_4} (CH_3CHO)^2$$

The overall activation energy will be about $2E_2 - E_9 - E_4$. For this energy expression the value obtained experimentally is (55 kJ/mole).

It can be observed that when branching takes place according to the Reaction 3a, the maximum rate is proportional to the square of initial aldehyde concentration; however, as Griffiths and Skirrow [10] have reported when Reaction 3 is the only branching step, the maximum rate is proportional to the three halves power of the initial aldehyde concentration. This may be explained as follows:

For long chains when the rate of peracid decomposition is slow relative to its rate of formation, i.e.

$$CH_3CHO + O_2 \rightarrow CH_3CO_3H$$

the rate equation will be

$$W = -d(O_2)/dt = K_2(K_3/2K_9)^{0.5} (CH_3CHO)(CH_3CO_3H)^{0.5}$$

or

$$W = K_2(K_3/2K_9)^{0.5} [(CH_3CHO)_{init.} - (CH_3CO_3H)] (CH_3CO_3H)^{0.5}$$

which is maximal when $dW/d(CH_3CO_3H) = 0$ i.e., when

$$K_2(K_3/2K_9)^{\frac{1}{2}} \left[\frac{1}{2}(CH_3CHO)(CH_3CO_3H)^{-\frac{1}{2}} - \frac{3}{2}(CO_3CH_3H)^{\frac{1}{2}}\right] = 0$$

Where

$$(CH_3CHO)(CH_3CO_3H)^{-\frac{1}{2}} = 3(CH_3CO_3H)^{\frac{1}{2}}$$

or

$$1/3(CH_3CHO) = (CH_3CO_3H)_{max.}$$

i.e., when 1/3 of the initial aldehyde has been used, the rate of reaction will be a maximum at a value of

$$W_{max.} = \frac{2K_2}{3\sqrt{3}} \left(\frac{K_3}{2K_9}\right)^{\frac{1}{2}} (CH_3CHO)^{1.5}$$

This expression is satisfied when branching is

governed by Reaction 3. The maximum rate can be expressed by the equation

$$W_{max.} = \frac{3\sqrt{3}}{16} K_2 \left(\frac{K_{3a}}{2K_9}\right)^{\frac{1}{2}} (CH_3CHO)^2$$

if Reaction 3a is assumed to be as the branching step.

As experimental observations show, the maximum rate depends on the 1.85 power of the initial acetaldehyde concentration which is closer to 2 rather than to 1.5, thus the branching step 3a seems to be more important. The difference between the values 1.85 (observed order) and two (predicted in the case of branching via (3a)) could be ascribed to the rate of initiation which cannot be ignored compared with the rate of branching [10]. Thus, as the observed order lies between 1.5 and 2, both branching steps 3 and 3a can be predicted. These considerations lead to an oxygen dependency of the rate even for the oxygen-rich mixtures as observed experimentally. If at low oxygen/fuel ratios, Terminations 8 and 10 are considered, the maximum rate will depend on the initial oxygen concentration since these termination steps compete with the propagation Reaction 1 for $CH_3C\dot{O}$ radicals.

As Combe, Niclaus and Letort [11] have reported, at low temperatures (below 100°C) the rate shows little dependence on the initial oxygen concentration and at 155°C even for high oxygen/fuel ratios, the rate is proportional to $(O_2)^{\frac{1}{2}}$. The effect of temperature increase on the oxygen dependence could probably be due to the thermal instability of acetyl radicals at higher temperatures (4a). Reaction 4a competes with the propagation step (1) leading to an oxygen dependent rate.

As a result, within the temperature range of these experiments (150-400°C) the maximum rate was found to depend on acetaldehyde to the power 1.85 and oxygen to the power 0.4.

Kinetically, the proposed mechanism is seen to be in reasonable agreement with the experimental observations.

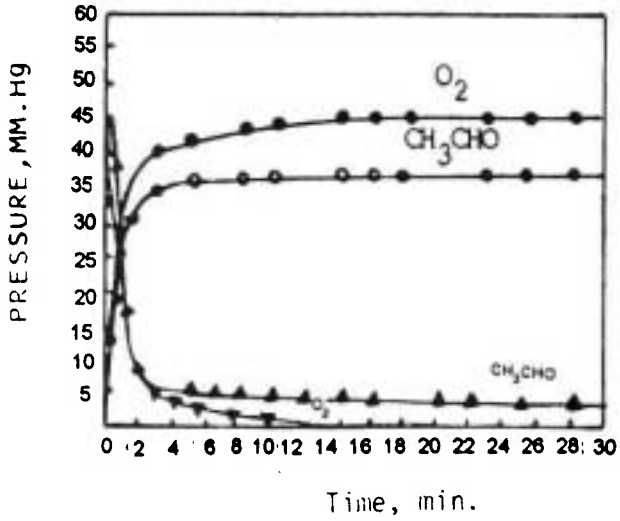

Figure 14. The variation of the reactants pressure with time in the oxidation of acetaldehyde. Initial CH_3CHO = 40 ; O_2 = 45 mm.Hg. at 300°C.

Kinetics Data

Figure 14 shows the partial pressures of unchanged acetaldehyde and oxygen and also the consumption of these reactants for a typical reaction. Figure 15 indicates the pressure-time variation at 300°C.

Under the conditions employed, the maximum

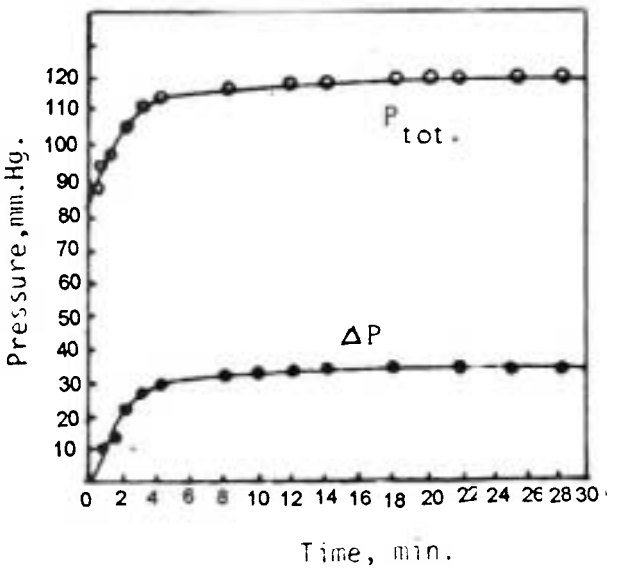

Figure 15. Pressure-time curves of the oxidation of acetaldehyde at 300°C. Initial CH_3CHO = 40 ; O_2 = 45 mm.Hg. Reaction vessel: clean pyrex glass dia. = 28.3 mm. vol. = 171 ml.

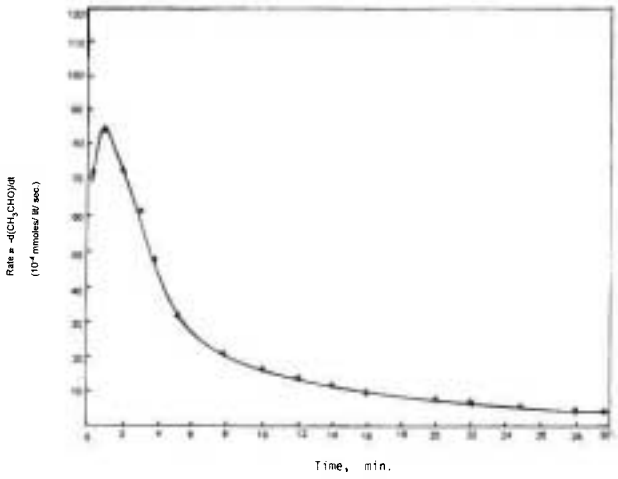

Figure 16. Variation of the reaction rate with time for the oxidation of gaseous acetaldehyde at 300°C. Initial $CH_3CHO = 40$; $O_2 = 45$ mm.Hg.

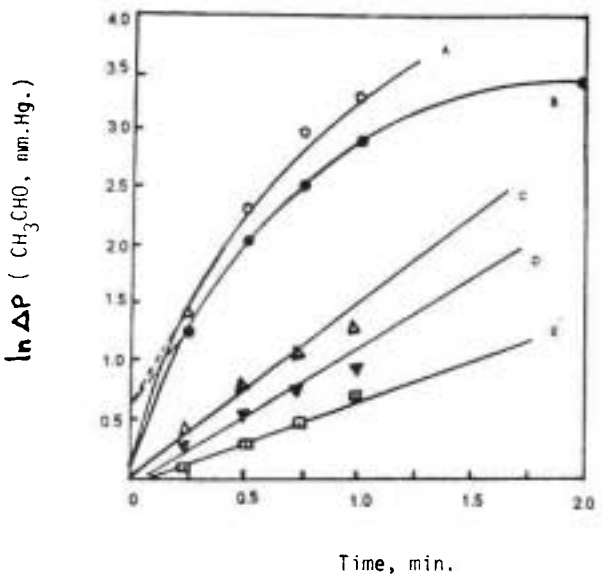

Curve	A	B	C	D	E
Initial fuel CH_3CHO (mm.Hg)	50	40	30	20	10

Figure 17. The variation of the logarithms of fuel presseure change with time for the oxidation of gaseous acetaldehyde at 300°C. Initial oxygen Pressure = 45 mm.Hg.

rate obtained (as the rate of acetaldehyde consumption) was 18.29 mm. Hg./min, which occurred at about 1 minute after the start of the reaction. The variation of the reaction rate with time which is plotted in Figure 16, shows an acceleratory portion, a maximum point and a decreasing portion. As the observed induction period was only about 1.5 seconds at the temperature of the oxperiment, the pressure change vs time curve can not depict this short period, although it does appear from the $\ln\Delta P(CH_3CHO)$-time diagram (Figure 17 curve B) for various initial pressures of acetaldehyde. The slope of the linear part of curve B (Figure 17) is 2.2 which indicates a net-branching factor $\phi = 2.2\ min^{-1}$ for the typical reaction ($CH_3CHO = 40$, $O_2 = 45$ mm Hg and T = 300°C). Table 3 gives the data used to compute the values of ϕ. A similar result is obtained from Figures 18 and 19. The maximum rate during the acceleration period occurred after consumption of 45.7% of the initial acetaldehyde which is in agreement with Semenov's hypothesis [12].

TABLE 3. Kinetic Data at Early Stages of Acetaldehyde Oxidation

Time (min.)	Used CH_3CHO (mm.Hg.) $(\Delta P)_1$	Produced m/e=60 (mm.Hg.) $(\Delta P)_2$	Log_e $(\Delta P)_1$	Log_e $(\Delta P)_2$	$-\frac{d[CH_3CHO]}{dt}$ (mm.Hg./min)	$\frac{d[M]}{dt}$ (mm.Hg./min)
0.25	3.00	0.79	1.25	-0.23	12.00	3.16
0.50	7.86	1.69	2.05	+0.53	15.72	3.38
0.75	12.98	3.61	2.55	+1.29	17.30	4.81
1.00	18.29	5.30	2.90	18.29	5.30	
2.00	31.29	7.36	3.43	+2.11	15.64	3.68

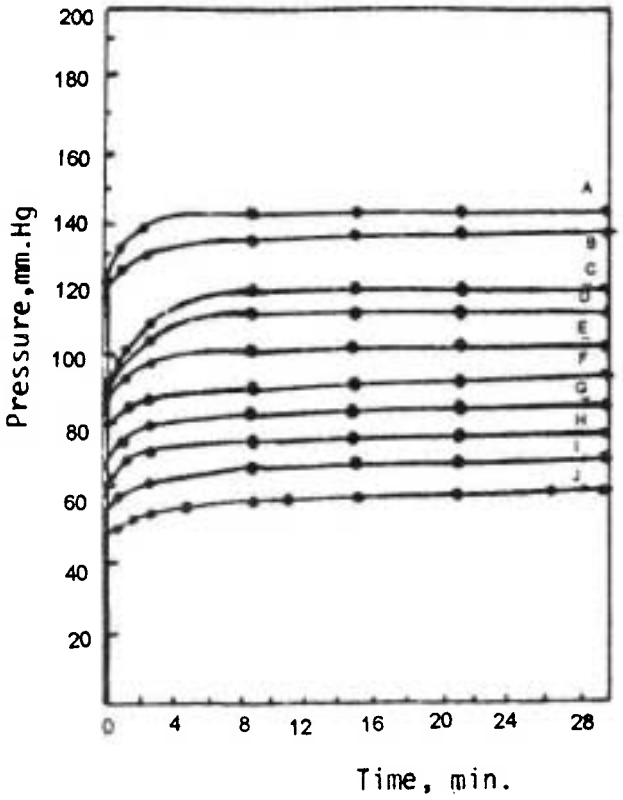

Curve	A	B	C	D	E	F	G	H	I	J
Initial fuel pressure mm.Hg.	50	45	40	35	30	25	20	15	10	5

Figure 18. Variation of the total pressure with time for the oxidation of acetaldehyde at 300°C and various initial fuel pressures. Initial O_2 = 45 mm.Hg.

Since the first portion of curve B (Figure 17) is a straight line having a slope of 2.2, it probably indicates that the pressure change of acetaldehyde during the initial stages of the reaction is an exponential function of the time, i.e. $\Delta P = Ae^{\phi t}$, in which A is a constant and ϕ is the net branching factor at 2.2 min^{-1} for the experimental conditions.

To study the effect of fuel pressure, two series of runs were carried out with the same initial oxygen pressure but using various acetaldehyde initial pressures at a temperature of 300°C. The results obtained showed that the reaction rate increases with an increase [13] in acetaldehyde pressure (Figure 18). For the second series of mixtures the acetaldehyde consumption values have been measured and plotted

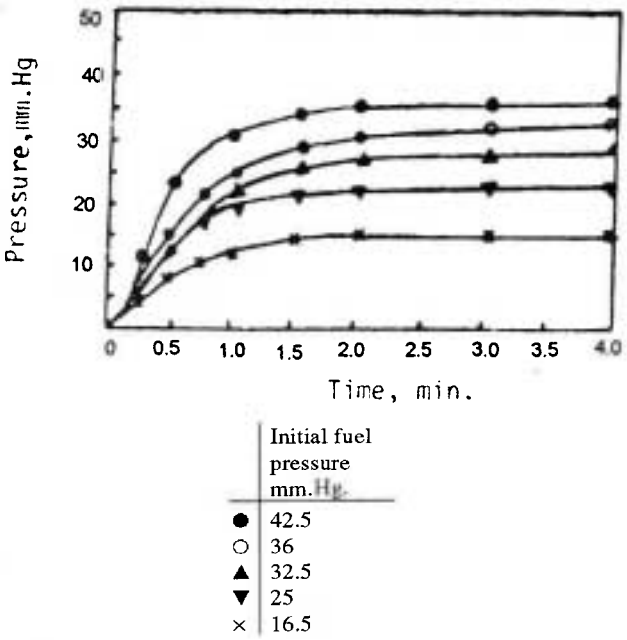

Figure 19. Variation of fuel consumption with time during the initial stages in the oxidation of acetaldehyde at 300°C. Initial O_2 = 45 mm.Hg.

against time (Figure 19).

A plot of the logarithm of maximum rate against the logarithm of acetaldehyde initial pressure is a straight line with a slope of 1.85, the reaction order for W_{max} with respect to acetaldehyde pressure

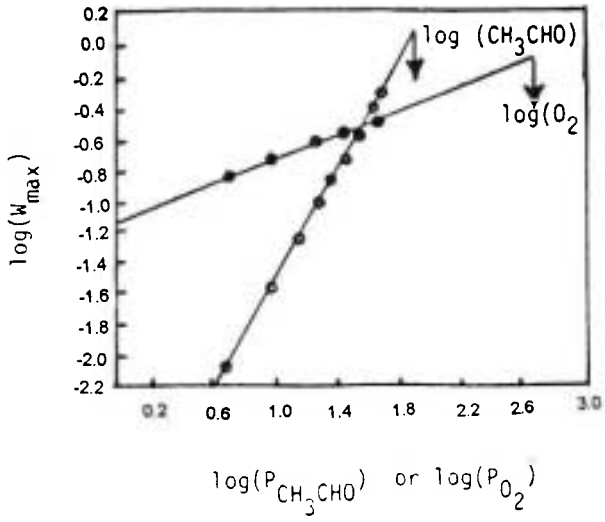

Figure 20. Variation of log (W_{max}) with log ($P_{reactants}$) at 300°C. ● Initial CH_3CHO = 40 mm.Hg. ; ○ O_2 = 45 mm.Hg.

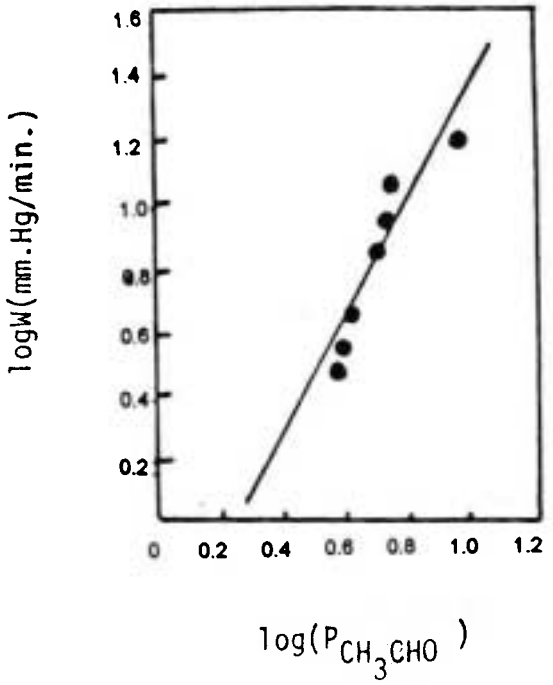

Figure 21. Variation of log (rate) with log (P_{CH_3CHO}) at 300°C. Initial O_2 = 45 ; CH_3CHO = 40 mm.Hg.

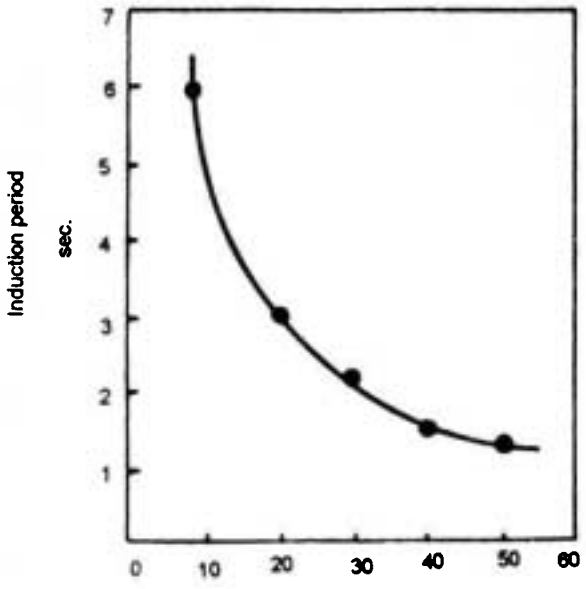

Figure 23. Variation of the induction period with fuel pressure.

(Figure 20, Tables 5 &6). This order was compared with the order of reaction with respect to time [14] which is equal to the slope of the line obtained in Figure 21. This order was 1.81. Both values are comparable with the results previously obtained [11, 15]. It is observed that the order with respect to time is slightly smaller than the order with respect to pressure; this indicates that the rate falls off more slowly than would be expected or the reaction is autocatalytic.

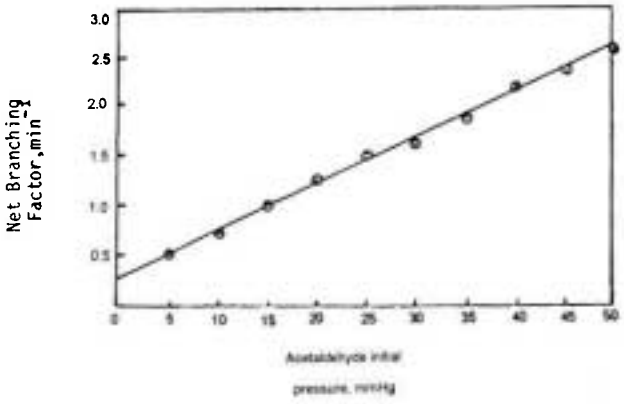

Figure 22. Variation of the net branching factor with initial acetaldehyde pressure at 300°C. Initial O_2 = 45 mm.Hg.

The variation of the net-branching factor with initial acetaldehyde pressure, which is plotted in Figure 22, is a straight line and extrapolates to a negative intercept on the horizontal axis. As a result, the Knox equation [16] $\phi = K_b\left[\frac{n\alpha K_P(Hy)}{K_t} - 1\right]$ does not quite fit the oxidation of gaseous acetaldehyde. The variation of the induction period τ with acetaldehyde pressure is shown in Figure 23 and as Table 4 indicates, a relatively constant value of $\phi\tau$ is obtained in agreement with Semenov's suggestion [12].

To investigate whether the reaction rate is influenced by the reactant concentrations or by their pressure in the reactor, a series of runs were carried out with constant acetaldehyde initial pressure and varying oxygen initial pressures; but the total pressure was held contant by adding the required amounts of oxygen-free nitrogen gas to initial mixtures (Tables 5 and 6). The results, which are plotted in Figure 24,

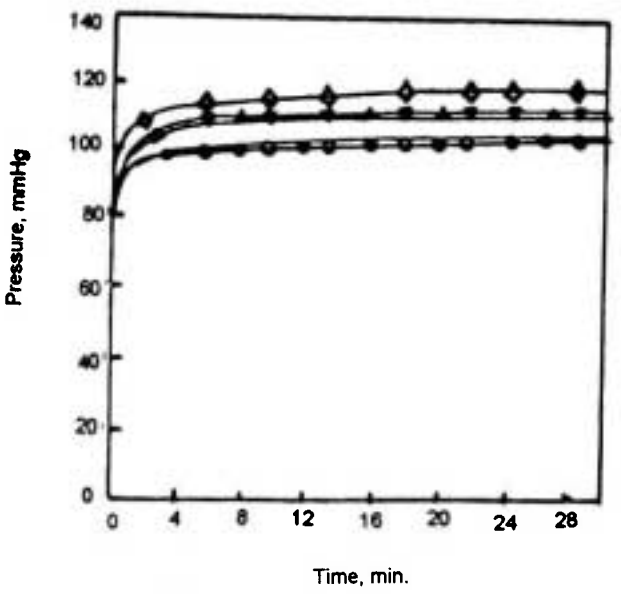

Figure 24. Variation of the total pressure with time in the oxidation of acetaldehyde at 300°C. Initial CH_3CHO = 40 mm.Hg. Initial O_2 : ○ = 5 , ● = 10 , Δ = 20 , Δ = 30 , ◇ = 40 mm.Hg.

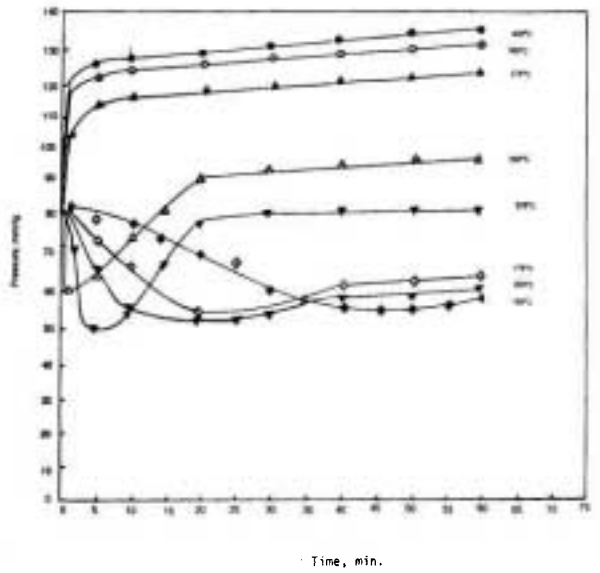

Figure 25. Pressure-time curves for the oxidation of gaseous acetaldehyde at various temperatures. Initial CH_3CHO = 40 ; O_2 = 45 mm.Hg.

show that the reaction order is 0.44 with respect to oxygen pressure which is close to the previously obtained order (.38) and indicates that the initial rate is independent of total pressure.

Thus, since the initial rate is independent of total pressure of the system, the order with respect to acetaldehyde is also due to itself and not to its pressure. The initial reaction rate equation becomes

$$-d[CH_3CHO]/dt = K[CH_3CHO]^{1.85} \times [O_2]^{0.4}$$

The reaction rate-temperature dependence of the oxidation process was studied over the range of 150-400°C. The pressure change, rate of reaction, activation energy, net branching factor and induction period have been characterised in the range of the work. The results obtained are summarised as follows:

a) the nature of the reaction products within the range studied was almost independent of temperature.

b) the time required for the reaction to proceed from 10% to 30% pressure change was measured on the chart recorder of the mass spectrometer at all temperatures studied. In the range of 150-250°C, the reaction was accompained by a pressure decrease (Figure 25) and the plot of the $\log \frac{1}{t_{30} - t_{10}}$ the reciprocal

TABLE 4. Variation of Induction Period τ with Acetaldehyde Initial Pressure.

Initial CH_3CHO (mm.Hg.)	5	10	15	20	25	30	35	40	45	50
ϕ (min^{-1})	0.51	0.70	1.00	1.25	1.53	1.64	1.88	2.20	2.39	2.57
τ (sec)		6		3		2.25		1.50		1.35
ϕτ		0.070		0.032		0.061		0.055		0.038

TABLE 5. The Effect of total Pressure on the Initial Rate

Initial reactants, mm.Hg.					
CH_3CHO	O_2	N_2 mm.Hg.	Initial rate (mm.Hg./min)	log P_{O_2}	log W
40	5	35	7.00	0.69997	0.84510
40	10	30	10.40	1.00000	1.01703
40	20	20	14.00	1.30103	1.14613
40	30	10	16.10	1.47712	1.20683
40	40	-	17.49	1.60206	1.24279

TABLE 6. The Effect of Oxygen Pressure.

O_2	CH_3CHO	Total press	order
variant	constant	variant	0.38
variant	constant	constnt	0.44

absolute temperatures was found to be approximately a straight line, which was slightly inclinded to a similar line obtained for the temperature range of 275-400°C (Figure 26) where the reaction was accompained by a pressure increase. The overall activation energies of 53.50 and 57.27 kJ mole^{-1} were computed for the two temperature ranges respcetivly.

c) the existence of an induction period τ at lower temperatures provides evidence for the accumulation of peroxides during the early stages of the oxidation process. The variation of log τ with reciprocal absolute temperature is plotted in Figure 27. The figure indicates an overall activation energy of 53.90 kJ mole^{-1} for the reaction over the whole temperature range.

d) the maximum rate-temperature plot is a curve

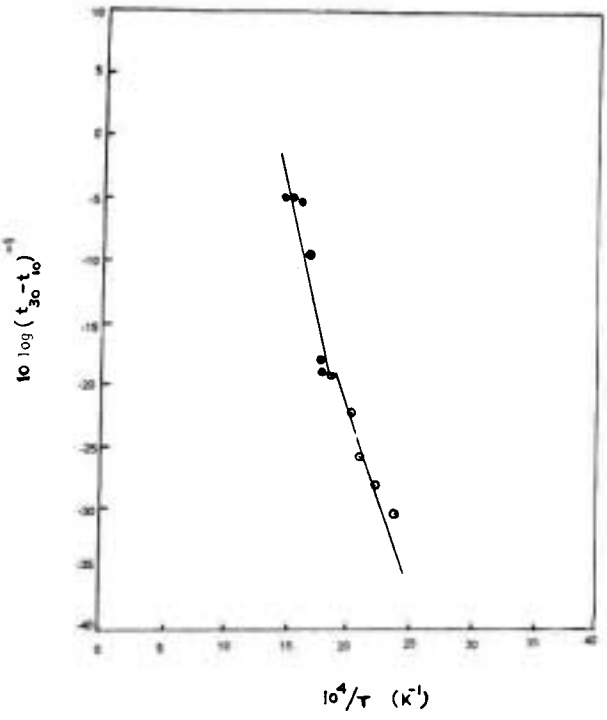

Figure 26. Variatin of $\log(t_{30} - t_{10})^{-1}$ with the reciprocal absolute temperature. Initial CH_3OH = 40 ; O_2 = 45 mm.Hg.

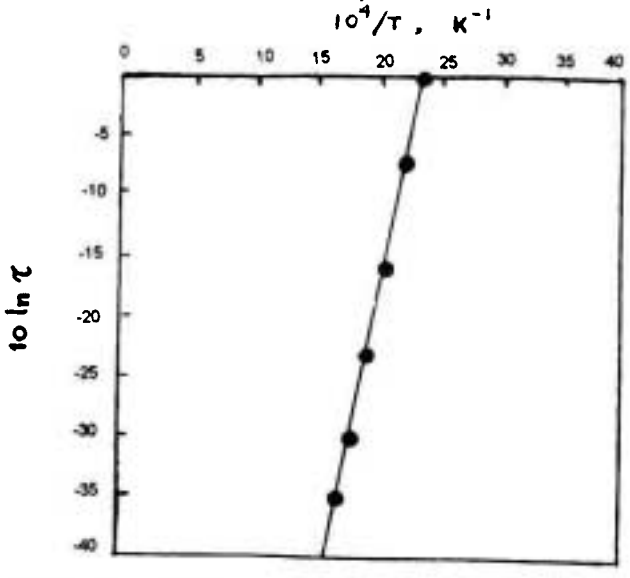

Figure 27. Variatin of log(induction period) with the reciprocal absolute temperature. Initial CH_3CHO = 40; O_2 = 45 mm.Hg.

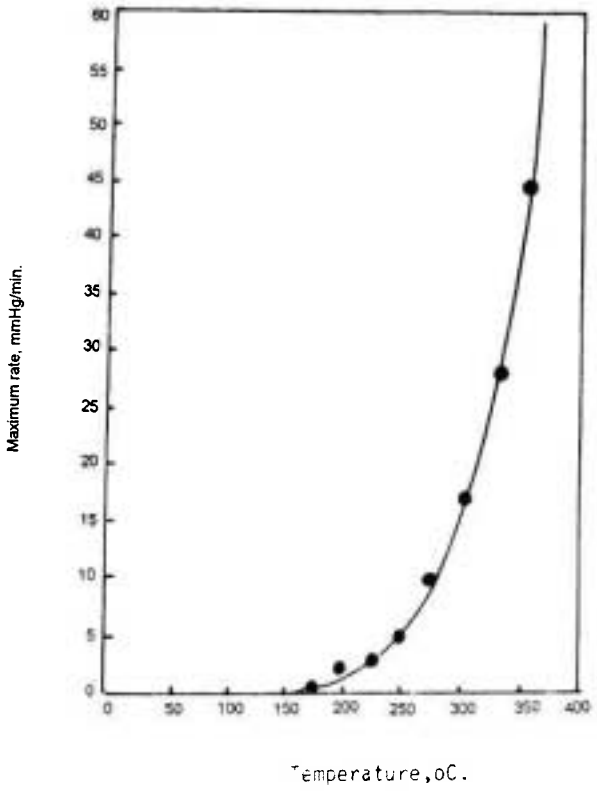

Figure 28. Variation of W_{max} with temperature in the gas-phase oxidation of acetaldehyde. Initial fuel = 40 ; O_2 = 45 mm.Hg.

the slope of which increases sharply at above 250°C (Figure 28).

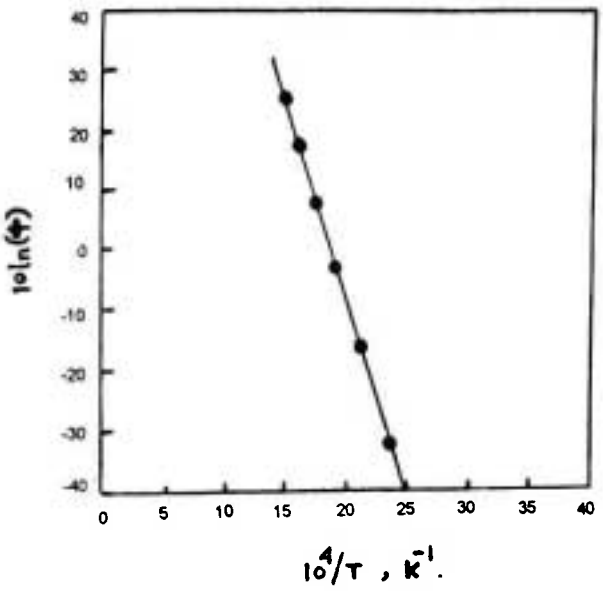

Figure 29. Net-branching factor-temperature dependence in the gas-phase oxidation of acetaldehyde. Initial CH_3CHO = 40 ; O_2 = 45 mm.Hg.

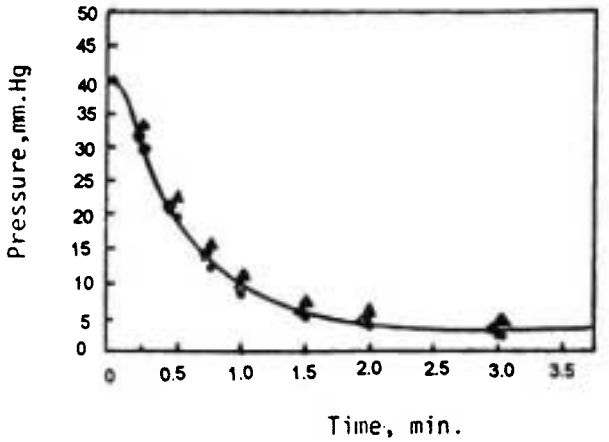

Figure 30. The plot of acetaldehyde partial pressure against time during the initial stages of acetaldehyde oxidation.

e) the net branching factor ϕ, changes with temperature of the reaction mixture as well as with pressure. The experimental observations indicate that for a certain oxidation mixutre of CH_3CHO/O_2, the value increases exponentially with temperature, i.e. $\phi \approx \exp.(-E/_{RT})$. If the variation of ϕ with initial pressure at constant temperature is taken into account, then $\phi \approx K\,[P_{CH_3CHO}]^{0.8}$ is obtained, (Figure 29) and it is concluded that the net branching factor fits the following relationship:

$$\phi = K[P_{CH_3CHO}]^{0.8}.\exp(-E/_{RT})$$

f) the addition of pure nitrogen, helium and argon gases has no effect on the rate of reaction. Figure 30 shows the partial pressure of acetaldehyde in the reaction mixture during the course of 4 minutes which is measured by the mass spectrometric analytical treatment. It is concluded that the inert gases have but a very small acceleratory effect on the oxidation rate of acetaldehyde, presumably as a result of a partial heterogeneous termination step.

g) other additives such as CO, CO_2, H_2 and H_2O gases (final products) have no effect on the reaction rate. This is in agreement with Minkoff and Tipper [1].

```
C      ****** Mass Sectral Analysis reaction Kinetics Data. ******
C      ****** Gas-Phase Oxidation of Acetaldehyde at 300° C ******
C      ************ CH3CHO=40 mm.Hg , O2=45 mm.Hg **************
       DIMENSION   H(14),P(14),HH(14),A(14,14),AA(14,14)
        DATA N/14/, AA /3*0.,6.06,4*0.,.89,4.37,9*0.,3.,8*0.,.67,14*0.
      +,1.58,14*0.,.75,14*0.,1.1,1.74,15*0.,.036,.05,8*0.,.39,6*0.
      +,7.21,14*0.,.013,14*0.,.062,.05,9*0.,2.,18*0.,.54,28*0./
       WRITE(1,33)
  33   FORMAT(20X,'Mass Sectral Analysis Reaction Kinetics Data.'/
      +20X,' Gas-Phase Oxidation of Acetaldehyde at  300' C '//
      +26X,'CH3CHO=40 mm.Hg , O2=45 mm.Hg'//38X,'h Valuse'/1X,85('-'))
       DO 44 I=1,N
  44   WRITE(1,55)(AA(I,J),J=1,N)
  55   FORMAT(1X,14F6.3/)
       WRITE(1,66)
  66   FORMAT(1X,85('-')//)
       OPEN (2,FILE='DATA.TXT',STATUS='OLD')
  77   READ(2,111)ITIME,(H(I),I=1,N)
       IF(ITIME.EQ.99)GOTO 200
 111   FORMAT(I2,14F7.3)
       DO 45 I=1,N
       DO 45 J=1,N
  45   A(I,J)=AA(I,J)
       DO 10 I=1,N
  10   HH(I)=H(I)
  7    DO 1 I=1,N
       ICONT=0
       DO 2 J1=1,N
       IF(A(I,J1).NE.0.) ICONT=ICONT+1
  2    CONTINUE
       IF(ICONT.NE.1)GOTO 1
       DO  3 J=1,N
       IF(A(I,J).EQ.0.)GOTO 3
       P(J)=H(I)/A(I,J)
       DO 20 I1=1,N
       H(I1)=H(I1)-A(I1,J)*P(J)
 20    A(I1,J)=0.
       GOTO 1
   3   CONTINUE
   1   CONTINUE
       ICONT=0
       DO 6 I=1,N
       DO 6 J=1,N
       IF(A(I,J).NE.0.)ICONT=ICONT+1
   6   CONTINUE
       IF(ICONT.NE.0)GOTO 7
       WRITE(1,8)ITIME,(HH(I),I=1,N)
       WRITE(1,9)(P(I),I=1,N)
   8   FORMAT(' TIME(MIN):',I2,' H:'14F7.3/)
   9   FORMAT(' P:'14F8.5//120('-'))
       GOTO 77
 200   END
```

Mass Sectral Analysis:Reaction Kinetics Data.
Gas-Phase Oxidation of Acetaldehyde at 300° C

CH3CHO=40 mm.Hg , O2=45 mm.Hg

h Values

.000	.000	.670	.000	.000	.000	.000	.000	.000	.000	.000	.000	.000	.000
.000	.000	.000	1.580	.000	.000	.000	.000	.000	.000	.000	.000	.000	.000
.000	.000	.000	.000	.750	.000	.000	.390	.000	.000	.000	.000	.000	.000
6.060	.000	.000	.000	.000	1.100	.000	.000	.000	.000	.000	.000	.000	.000
.000	.000	.000	.000	.000	1.740	.000	.000	.000	.000	.000	.000	.000	.000
.000	3.000	.000	.000	.000	.000	.000	.000	.000	.000	.000	.000	.000	.000
.000	.000	.000	.000	.000	.000	.036	.000	.000	.000	.000	.000	.000	.000
.000	.000	.000	.000	.000	.000	.050	.000	.000	.000	.000	.000	.000	.000
.890	.000	.000	.000	.000	.000	.000	.000	.000	.000	2.000	.000	.000	.000
4.370	.000	.000	.000	.000	.000	.000	7.210	.000	.000	.000	.000	.000	.000
.000	.000	.000	.000	.000	.000	.000	.000	.013	.000	.000	.000	.000	.000
.000	.000	.000	.000	.000	.000	.000	.000	.000	.062	.000	.000	.000	.000
.000	.000	.000	.000	.000	.000	.000	.000	.000	.050	.000	.000	.000	.000
.000	.000	.000	.000	.000	.000	.000	.000	.000	.000	.000	.540	.000	.000

TIME(MIN): 1 H:	.000	.000	.000	.000	.000	.000	.040	.055	.000	.000	.000	.005	.004	.000
P:	.00000	.00000	.00000	.00000	.00000	.00000	1.11111	.00000	.00000	.08065	.00000	.00000	.00000	.00000
TIME(MIN): 2 H:	10.000	34.000	27.960	56.750	13.100	22.500	.085	.117	11.000	149.000	.046	.009	.007	3.780
P:	7.99808	7.50000	14.92537	21.51899	29.05460	7.52874	2.36111	15.81808	3.53846	.14516	1.94085	7.00000	.00000	.00000
TIME(MIN): 4 H:	11.200	39.500	29.710	50.430	12.700	12.000	.075	.105	10.030	163.600	.053	.014	.120	4.000
P:	6.99691	4.00000	16.71642	25.00000	30.01940	7.29885	2.08333	18.44986	4.07692	.22581	1.90138	7.40741	.00000	.00000
TIME(MIN): 6 H:	11.400	41.900	31.470	38.110	12.300	9.000	.054	.075	9.150	166.800	.050	.029	.023	3.890
P:	5.00563	3.00000	17.01493	26.51899	31.50768	7.06897	1.50000	20.10061	3.84615	.46774	2.34749	7.20370	.00000	.00000
TIME(MIN): 8 H:	12.000	44.240	38.690	36.200	12.200	7.500	.034	.047	8.880	171.500	.040	.022	.018	3.890
P.	4.70088	2.50000	17.91045	28.00000	40.69933	7.01149	.94444	20.93719	3.07692	.35484	2.34811	7.20370	.00000	.00000
TIME(MIN):10 H:	12.000	45.500	33.180	34.890	12.000	6.000	.012	.020	8.700	174.700	.036	.019	.015	3.890
P:	4.50558	2.00000	17.91045	28.79747	33.06032	6.89655	.33333	21.49939	2.76923	.30645	2.34502	7.20370	.00000	.00000
TIME(MIN):12 H:	12.000	47.400	33.600	32.880	11.800	6.000	.011	.015	8.440	175.300	.025	.014	.011	3.890
P:	4.19476	2.00000	17.91045	30.00000	33.47908	6.78161	.30556	21.77100	1.92308	.22581	2.35333	7.20370	.00000	.00000
TIME(MIN):14 H:	12.000	49.000	34.120	31.780	11.800	6.000	.009	.012	8.260	176.500	.008	.014	.011	3.890
P:	4.01324	2.00000	17.91045	31.01266	34.02866	6.78161	.25000	22.04745	.61538	.22581	2.34411	7.20370	.00000	.00000

NOMENCLATURE

m/e	Mass to charge ratio
[A]	Concentration of specises A
W	Reaction rate
W_{max}	Maximum rate
RH	Hydrocarbon
K	Rate constant
t	Time
ΔP	Pressure change
ϕ	Net branching factor
τ	Induction period
E	Activation energy
T	Absolute temperature

REFERENCES

1. G. J. Minkoff and C. F. H. Tipper, "Chemistry of Combust. Reac.", Butterworths, London (1962).
2. A. J. B Robertson, "Mass Spectrometry", Methauen & Co., N. Y. (1954).
3. American Pet. Inst. Res. Proj. Mass spectral data.
4. R. M. Hohnson and I. W. Seddigi, "The Determination of Organic Peroxides", Pergamon Press, London (1970).
5. J. A. Kerr, *Chem. Rev.*, **66**: 465 (1966).
6. K. C. Salooja, *Combust. Flame*, **9**: 219 (1965).
7. L. P. Blanchard, J. B. Farmer and C. Ouellet, *Canadian J. Chem.* **35**: 115 (1957).
8. N. A. Sokolova, A. M. Markvich and A. B. Nalbandyan, *Russ. J. Phys. Chem.* **35**: 415 (1961).
9. V. Caprio, A. Insola and P. G. Lignola, *Combust. Flame*, **35**: 215-224. (1984).
10. J. F. Griffiths and G. Skirrow, *Oxid. and Combust. Rev.*, **3**: 47 (1968).
11. A. Combe, M. Niclause and M. Letort, *Rev. Inst. France. Petrole*, Ann. Combust. Liq., **10**, 786, 929 (1955).
12. N. N. Semenov, "Some Problems of Chemical Kinetics and Reactivity", Vol. Iand II, Pergamon press, LONDON (1958).
13. P. Gray, J. F. Griffiths, S. M. Hasko and P. G. Lignola, *Combust. Flame*, **43**: 175-186 (1981).
14. K. J. Laidler, "Reaction Kinetics", Vol. I, Pergamon press, Oxford (1963).
15. A. Hardacre, G. Skirrow and C. F. H. Tipper, *Combust. Flamce*, **9**: 53 (1965).
16. J. H. Knox, *Trans. Farad. Soc.*, **55**: 1362 (1959).